

Compressive Behaviour of Filament Wound Steel/Carbon Hybrid Composites Tube

N. A. Jamaluddin, S. Abu Hassan*, U. Abdul Hanan, M.A. Md Amin and M. A. Mohd Adam

Faculty of Mechanical Engineering, Universiti Teknologi Malaysia, 81310 Skudai Johor, Malaysia
*shukur@utm.my

B. Omar
Department of Structure and Materials, Faculty of Civil Engineering, Universiti Teknologi Malaysia, 81310 Skudai, Johor, Malaysia

ABSTRACT

Fibre composites have been introduced in the automotive and aerospace applications due to their strength to weight ratio advantage to replace traditional engineering materials. However, due to automotive occupants' safety risks during collision, numerous studies have been done by researchers on the energy absorption capability of composites structures. Typically, advanced polymer composites have low specific energy absorption compared to traditional engineering materials due to low modulus and limited plastic behaviour. In this research, the effect of hybrid filament wound hexagonal tube made of high strength steel wire and carbon fibre/epoxy composites under compression was studied through laboratory testing. Two test samples, namely, carbon fibre composites (CCC) and carbon fibre/steel hybrid composites (CSC) hexagonal tubes were prepared using filament winding technique. The cured samples, then have cut to two different lengths, 40 mm and 45 mm for each respective sample. The results show that both CCC samples are able to absorb higher energy compared to CSC samples. However, in terms of specific energy absorption, the value for CSC samples are 9.37 % and 6.39 % higher than CCC samples for 40 mm and 45 mm sample length respectively. This indicates that the addition of metal is effective in increasing the energy absorption capability and strength to weight ratio of composites, which are an advantage in the automotive industry.

Keywords: *composites; crashworthiness; energy absorption; filament winding.*

Introduction

Polymer composites are specifically used in applications for automotive and aerospace industries. In order to reduce weight, traditional metals are frequently being replaced by lighter and strong polymer composites as materials for vehicle parts and components. Weight reduction of a vehicle is very important because vehicle weight directly affects its energy consumption [1]. A carbon fibre polymer composite (CFRP) has been used widely throughout the world as the replacement material with an average growth rate of 12 % for the last 23 years [2]. On top of being light-weight, CFRP also exhibits higher specific strength and rigidity compared to traditional metals. However, there is an increased concern in occupant safety risk during roadway accidents which leads to further analysis on the ability of polymer composites in terms of strength and energy absorption.

Compressive strength plays an important role in impact produced by collision between deformable bodies. The compressive strength of carbon fibre winding angle at 45° is 98 MPa [3], while compressive strength for steel is 170 to 310 MPa. This shows that carbon fibre is comparable to withstand higher compressive load compared to steel. However, carbon fibres composites show almost perfect brittle type failure mode which resulting them to fail at a very low strain [4]. Plus, the sheet-like aggregations readily allow the propagation of cracks. In other words, carbon fibres do not deform much and fail suddenly and catastrophically compared to steel.

A new structural material can be formed by combining two materials with different properties by taking into account the energy absorption capability. Schultz [5] determined one important parameter in the energy absorption study is the energy absorbed per unit mass of a crushed structure material, often called as the specific energy absorption (SEA). This parameter also indicates the strength to weight ratio of a material. In his research studied on the effect of geometry towards the “crashworthiness” of a structure, which is defined as the ability of a structure to absorb impact energy and survive impact during collision. Crashworthiness is concerned with energy absorption through controlled failure mechanisms and modes which enable the maintenance of a gradual decay in the load profile during absorption.

Nowadays, several studies have been carried out to determine the effects of various variables on the energy absorption capability of a composite tubes such as hybrid material by Huang et al. [6] and geometry shape by Palanivelu et al. [7] and Eshkoor et al. [8]. On the other hand, Ochelski and Gotowicki [9] and Elgalai et al. [10] focused on the effect of fibre reinforcement while Warrior et al. [11] studied the effect of boundary

condition on the energy absorption capability of a composite tube. In a more recent study, Alkbir et al. [12] analysed the effect of geometry and load-carrying capacity of hexagonal composites tubes on the crashworthiness parameters. In a similar research, a study on the crashworthiness parameters in composite material tubes made from natural fibres have been carried out by Eshkoo et al. [13]. They concluded that different trigger configurations could cause significant differences in the crashworthiness parameters and failure patterns of the composite tubes. Based on the previous studies mentioned above, they lack one important parameter that should be taken into consideration which is crush force efficiency. Helaili et al. [14] measured the crush force efficiency which is defined as the ratio of the average collapse load to the limit load of the structure and its effectiveness towards energy absorption capability of a structure. It is a useful measure of the uniformity of collapse load and for an ideal energy absorption structure, the ratio must be near or equal to one.

Other than that, Ha and Jeong [15] and Sapuan et al. [16] studied the crushing behaviour of a structure involving a variety of parameters such as fibre angle, structure geometry and different types of layer where the samples were fabricated using filament winding technique. Although numerous techniques existed, both researchers agreed that filament winding has matured to become one of the major manufacturing processes in the fabrication of high performance fibre reinforced composites. The effect of winding angle had also been studied by Misri et al. [17] which indicated that the value of energy absorption for 45° winding angle sample was higher compared to 90°. Similar statement was given by Abu Bakar [18] where samples with 45° winding angle had higher percentage in energy absorption compared to 30° and 80°. Resin is also one of the factors affecting the strength of a composite. In fibre reinforced composites fabrication, epoxies are always chosen as a binder due to their relatively high modulus and low shrinkage during curing.

This paper presents the experimental results of a study to investigate the compressive behaviour of filament wound composites tubes. The study involved two different composite systems, i.e. fully carbon and carbon/steel hybrid with epoxy matrix composites. The effect of tube lengths are also analysed and discussed in relation to energy absorption capability.

Methodology

Sample Preparation

Test samples were produced by winding high strength steel wire with diameter of 0.1 mm supplied by KISWIRE and T700 carbon fibre tows onto hexagonal

tubes using four-axes Entec filament winding machine located in Centre of Advanced Composite Materials (CACM), Universiti Teknologi Malaysia. In this filament winding technique, both reinforcing materials together with Sikadur 330 epoxy were wound onto a rotating mandrel with a fixed winding angle. A schematic diagram of the filament winding technique is shown in Figure 1. The shape of the tube was determined by the shape of the mandrel itself.

In this study, a hexagonal tube with cross section geometry size as shown in Figure 2 was produced. Two samples had been produced, namely CCC and CSC. CCC is the three layers carbon fibre tows, one after another, while during the fabrication of CSC, the second layer fibre was replaced by steel wires. A winding angle of 45° was chosen due to its optimal compressive strength based on literature by previous researchers [16, 17].

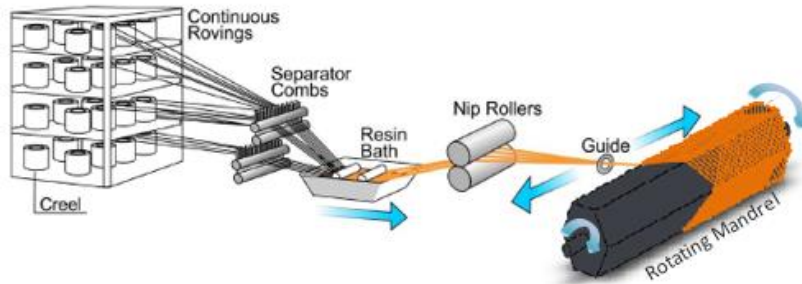


Figure 1: Schematic diagram of Filament winding technique

Sikadur 330 epoxy was used as the matrix and mixed with hardener to 4:1 ratio. This epoxy matrix was chosen due to its relatively high moduli and low shrinkage which is directly affected the compressive strength of the composites itself, Mokhtar et al. [3]. The sample was left to be fully cured for 24 hours at room temperature before demoulded. The cured sample was pulled out from the mandrel by using hydraulic pump that attached to a special designed jig.

The test sample was cut into hexagonal tubes with two different lengths of 40 mm and 45 mm respectively as shown in Figure 3(a). Three specimens are produced for each sample (i.e. CCC40, CSC40, CCC45, and CSC45) for further compression test preparation. The upper and lower ends of the test samples were trimmed and attached with strain gauges type FCA-1-11 of 1 mm gauge length and $120 \pm 0.5 \Omega$ gauge resistance.

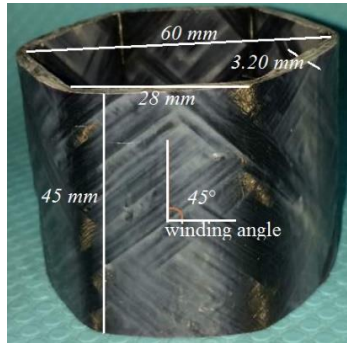


Figure 2: Hexagonal tube with cross section geometry

Compression Test

Compression test provides a standard method of obtaining data for research and development, quality control, acceptance or rejection under specifications and special purposes. From the test shown in Figure 4, the behaviour of the core, maximum load, compression strength, modulus, extension, strain and energy absorption of the core can be measured and analysed.

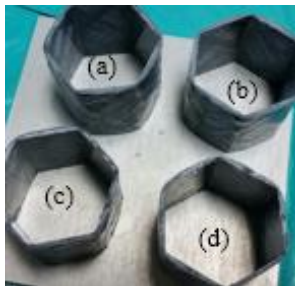


Figure 3: Samples for a) CCC45, b) CCC40
c) CSC45 and d) CSC40



Figure 4: Specimen under compression

The compression test is conducted using universal testing machine INSTRON 600 kN according to ASTM D695. The test specimen is placed between the steel platens and loaded at a quasi-static loading rate of 1mm/min, which generate an engineering strain rate of $6.7 \times 10^{-4} \text{ s}^{-1}$. All the cores are tested until it reaches 90 % of delamination.

Results

The results of the compression test are shown in the forms of load versus displacement and stress versus strain curves. The load versus displacement curves of CCC40 and CSC45 samples are presented in Figures 5 and 6 respectively. The load versus displacement curve of CCC40 as shown in Figure 4 increases linearly until the initial crushing at the first peak of 20.57 kN at 1.6 mm displacement. At this stage, the matrix cracking was initiated at the top end of the test sample where the crack propagation and matrix cracking started. Subsequently, the load versus displacement curve drops to -3.24 kN at displacement of 13.34 mm. This occurs due to matrix cracking and crack propagation. The negative value indicates the instability of the test specimen under compression load before the load increases to the compacting zone. Meanwhile, for CCC45, the peak load is 29.29 kN before decreasing to 2.76 kN at displacement of 9.22 mm. During the compression test, the specimen started to shear off and as the loading kept progressing, the shearing fracture became more obvious when the specimen entered the compact mode as the load increased up to failure.

Figure 6 shows the load versus displacement curves for CSC40 and CSC45 tubes. The curves increase non-linearly prior to the onset of matrix micro-cracking initiated at the ends of the tube. Basically, the deformation of the tube occurred in three stages for CSC40. In the first stage, the load increased until it reached the peak load value of 13.82 kN. During the second stage, the load dropped drastically before it reached the third stage where a fluctuated load occurred due to the existence of steel material which provided some plastic behaviour to the tube. The CSC45 produced similar results, but in the third stage, rather than a fluctuated load, a more or less constant force called the 'plateau force', F_{pl} occurred. This was also due to the presence of steel as a ductile material in the composites hexagonal tube.

A combined diagram of load versus displacement curves for CCC and CSC are shown in Figures 7 and 8. Both CCC and CSC samples behaved linearly at first stage and the axial load was absorbed as an elastic strain energy in the material. However, the elastic slope for CCC sample is greater than CSC, as can be seen from graph. Modulus of elasticity is a measure of the ability of a material to deform under lengthwise tension or compression. Therefore, material with a higher value of modulus of elasticity, which is CCC in this case, is stiffer and also able to withstand higher load.

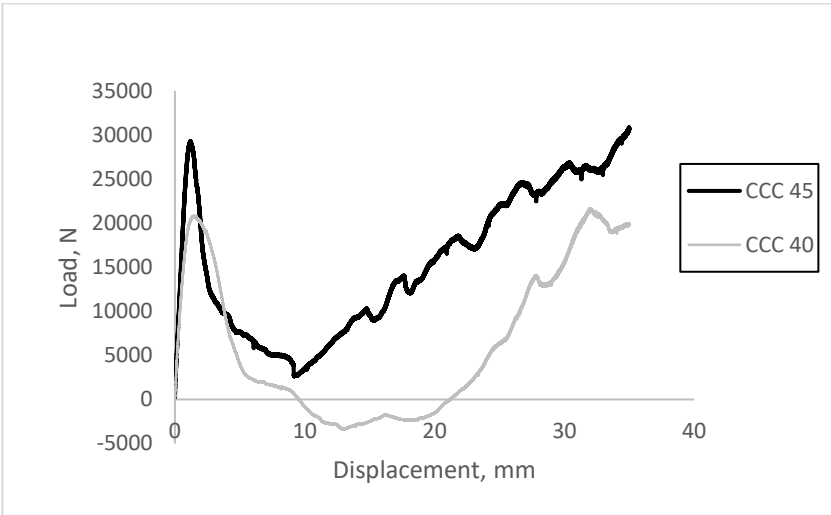


Figure 5: Load versus Displacement graph for CCC40 and CCC45

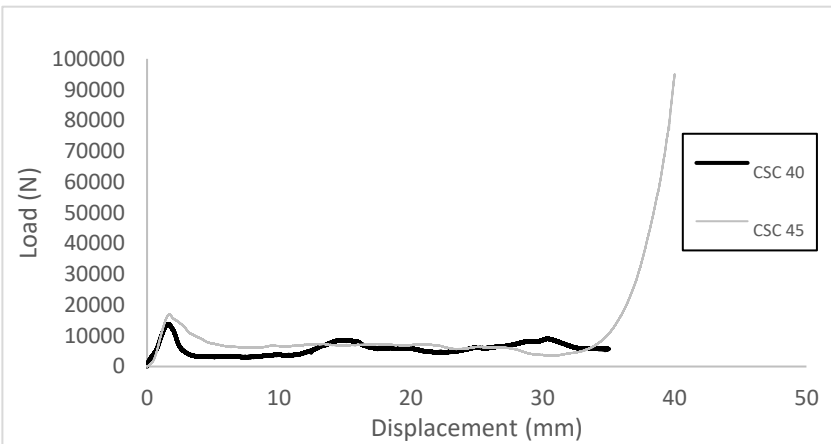


Figure 6: Load versus Displacement graph for CSC40 and CSC45

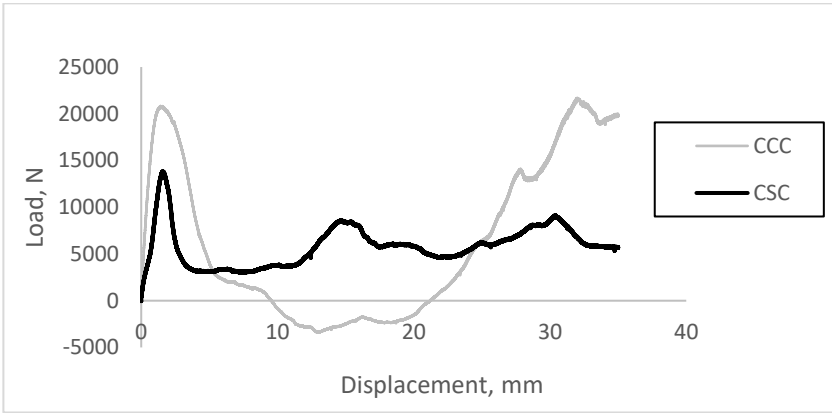


Figure 7: Load versus Displacement graph for CCC40 and CSC40 samples

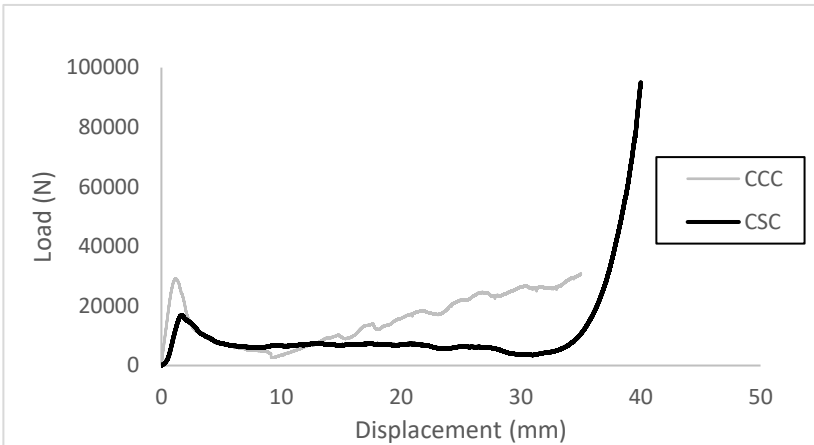


Figure 8: Load versus Displacement graph for CCC45 and CSC45 samples

The values of compressive modulus can be calculated from the gradient of the stress versus strain curves shown in Figures 9 and 10. These data are presented in Table 1. By referring to the presented data, it is clear that the compressive modulus values of CCC samples are greater compared to CSC samples, i.e. 294.77 MPa for CCC40 compared to 184.86 MPa for CSC40 and 511.61 MPa for CCC45 compared to 254.43 MPa for CSC45. Even though CCC samples were able to withstand higher loads, they fail catastrophically upon reaching the peak load and this can be seen from the load versus

displacement curves for both 40 mm and 45 mm samples. Catastrophic failure modes are not of interest in the design of crashworthiness structures. They occur when unstable interlaminar or intralaminar crack growth occurs in a long thin walled tube due to column instability. As a result, the actual magnitude of specific energy absorbed is much less and the peak load is too high to prevent injury to the occupants. For crashworthiness study, the crush modes of CCC40 and CCC45 are shown in Figure 11.

Meanwhile, in contrast to CCC samples, CSC samples had undergone progressive failure modes. The tube wall was torn during the compression test and while the inner side wall was buckling to the interior of the tube, the external side was buckling to the outside. Buckling occurred due to the increase of stress in the undamaged part of the tube. After exceeding allowable stress, cracks appeared in several places along the tube length accompanied by acoustic effects.

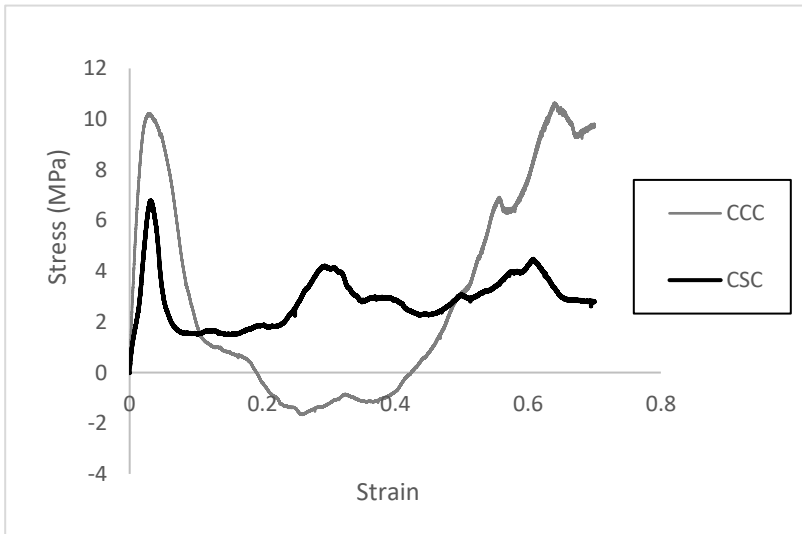


Figure 9: Stress versus Strain Graph for CCC40 and CSC40 samples

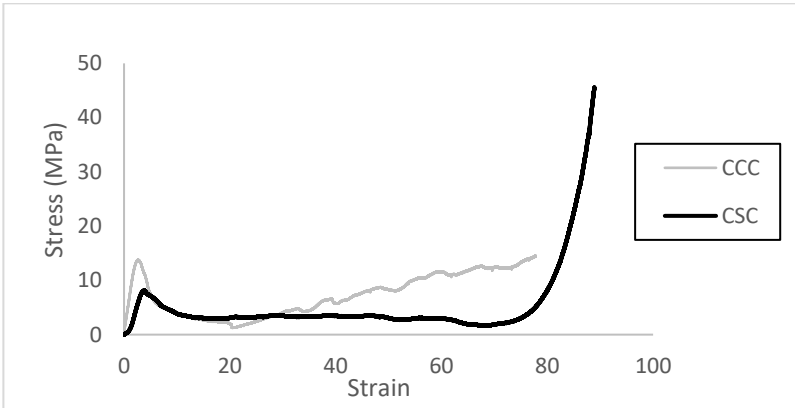


Figure 10: Stress versus Strain Graph for CCC45 and CSC45 samples

Table 1: Test samples Compressive Modulus

Sample	Compressive Modulus, MPa
CCC40	294.77
CSC40	184.86
CCC45	511.61
CSC45	254.43

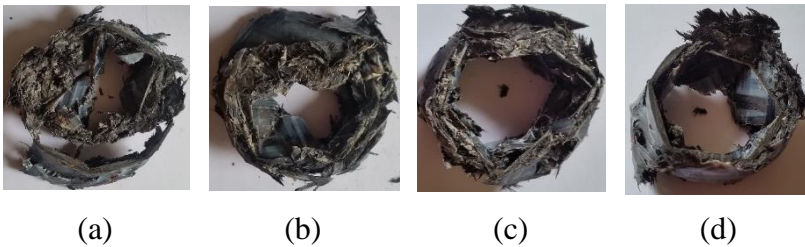


Figure 11: Crush Mode (a) CCC45 (b) CSC45 (c) CCC40 (d) CSC40

Discussion

Peak and average load

Load versus displacement curve shows the behaviour of crushing for a related tube. Crushing starts at a critical value which is called peak load and progressively deforms along the tube. From the load versus displacement curves shown in Figures 7 and 8, an average compressive load (\bar{P}) for each tube is calculated from the related load versus displacement. The summary of results for all the test samples are presented in bar chart shown in Figure 12. From the chart, it can be seen that the values of both peak load and average load of CCC samples are higher compared to CSC samples of the same length. The peak load values of CCC40 and CSC40 are 20.57 kN and 13.82 kN respectively, while for CCC45 and CSC45, the peak load values are 29.29 kN and 16.91 kN respectively. These peak loads are directly related to the compressive modulus of the tubes as CCC samples with higher compressive values are able to withstand larger loads compared to CSC samples. However, the differences in average loads between CCC and CSC samples are smaller which indicate that their energy absorption abilities are almost the same. Another observation that can be made from the chart is that the peak load is dependent on the tube's length. Figure 12 clearly indicates that the length of the tube significantly affects the peak load. From the results, it can be concluded that samples with longer lengths provide more resistance under compression load, and achieve higher values of peak and average loads.

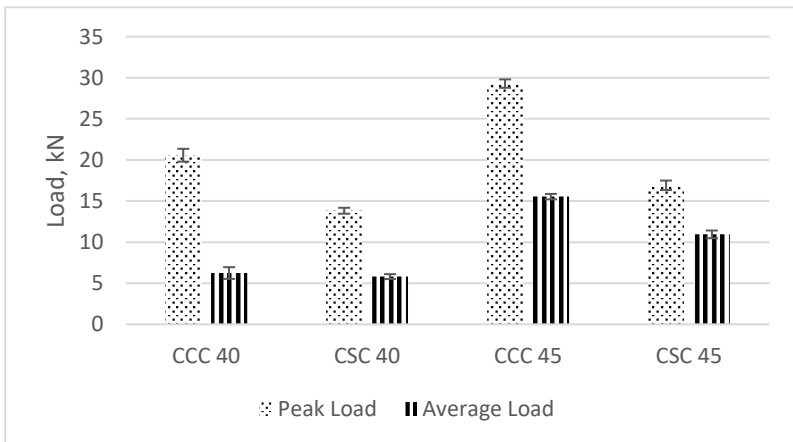


Figure 12: Peak Load and Average Load for different sample

Crush Force Efficiency

Another important parameter in the measure of crush performance is the crush force efficiency, which is defined as the ratio of the mean crush average load to the initial crush failure load. In order to evaluate the crashworthiness of energy absorber device, attention should be directed to its crush force efficiency. It is a useful measure of the uniformity of collapse load and for the ideal energy absorber, the value of the efficiency is equal to 1. The comparison of crush force efficiency between samples is depicted in Figure 13. The ratio of average load to peak load is the value to be considered to determine the failure mechanism of composite, namely catastrophic or progressive failure. In contrast to progressive failure, catastrophic collapse mode is defined by a lower value of crush force efficiency, as a result of a high value of peak load and a much lower value of average load during the compression test. From the chart, it is clearly shown that the CSC has higher crush force efficiency than CCC with a value of 0.42 and 0.65 for CSC40 and CSC45 compared to 0.30 and 0.53 for CCC40 and CCC45 respectively. This shows that CSC is more efficient to be used for energy absorption applications. Not to mention, efficiency also increases as the length of the tube increases.

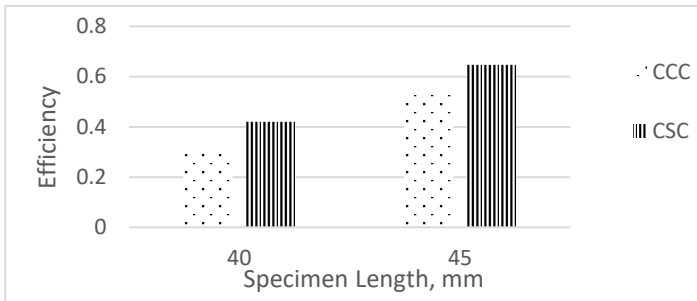


Figure 13: Comparison between samples group on crush force efficiency

Energy Absorption and Specific Energy Absorbed

The more efficient and effective method in limiting loads is to absorb or dissipate energy rather than to store it. The value of energy absorption capability of a structure is dependent on the area under the load versus displacement curve. Energy absorption values for all test samples are calculated from the respective curves and presented in Table 2.

From Table 2, it shows that CCC45 sample absorbs the highest energy

with a value of 545.52 J. On the other hand, for CSC45, the value is lower compared to CCC45 as the higher load resisted by CCC45 makes its area under the curve larger compared to CSC45, which also experienced a long plateau force. The same goes for the 40 mm length samples where the value of energy absorbed by CCC40 is higher compared to CSC40 with the value of 159.44 J and 125.17 J respectively. As for the difference in lengths, tubes with longer length are able to absorb more energy due to the longer crush effective length as a mean of energy absorption during compression.

Table 2: Value of Energy Absorbed for different samples

<i>Sample</i>	<i>Energy Absorbed (J)</i>
CCC40	159.44
CSC40	125.17
CCC45	545.52
CSC45	438.46

Consequently, tubes with higher value of average crushing load also show higher value of energy absorption due to their longer distance in the post crushing zone.

Weight of structures also plays an important role particularly in the automotive industry where the fuel consumption is directly related to vehicular weight. The specific energy absorption is defined as energy per unit mass of a material and the mass of every sample is shown in Table 3, where it can be seen that the CSC samples are lighter compared to CCC.

Table 3: Value of Mass for different sample

<i>Sample</i>	<i>Mass (g)</i>	<i>Mass (kg)</i>
CCC40	26	0.026
CSC40	18.5	0.019
CCC45	28	0.028
CSC45	21	0.021

Using the value of mass and energy absorbed by the tubes, specific energy absorbed for all samples can be calculated, as presented in Figure 14. The chart shows that the specific energy absorbed value for CSC samples are higher compared to CCC samples where the value of 6766.18 J/kg and 20878.99 J/kg are calculated for CSC40 and CSC45, while 6132.26 J/kg and 19482.75 J/kg are calculated for CCC40 and CCC45 respectively. Therefore, it can be concluded that CSC samples exhibit higher strength to weight ratio.

It is also important to note that the effect of tube length can be eliminated when comparing the specific energy of the tubes.

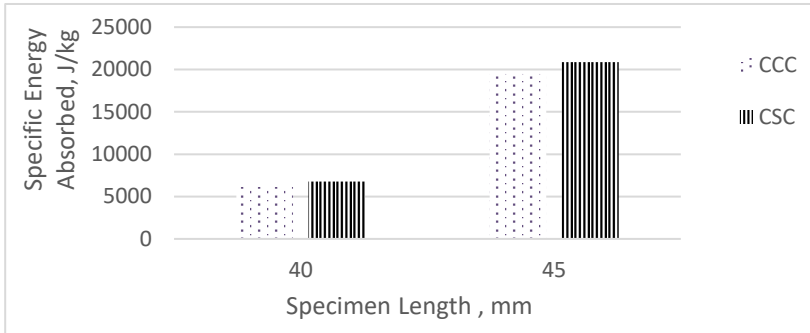


Figure 14: Comparison between samples group on Specific Energy Absorbed

Mean crushing stress is defined as the mean crushing load divided by the cross-sectional area, which is not a material characteristic, but a structural dependent value. For example, according to Mamalis et al. [19] in their paper on crashworthy capability of composite material structures, the mechanism controlling the crushing process is dependent on the rate of applied stress. Therefore, it can be said that the crush stress is an important criterion in crashworthiness. Meanwhile, Barnes [20] in his paper of crash safety assurance not only stated that the crushing stress in composite structures is an important parameter that is dependent on material and geometric parameters, but he also added that when designing an energy absorbing structure using composites, the mean crushing stress is a critical design parameter that must be known. Besides, the mean crushing stress is found to be considerably lower than the compressive strength.

The value of mean crushing stress for each sample is tabulated in Table 4. From the data shown in Table 4, the value of mean crushing stress for CCC samples are higher compared to CSC samples with the value of 2.96 MPa for CCC40 and 7.36 MPa for CCC45, and 2.75 MPa for CSC40 and 5.19 MPa for CSC45. Another comparison that can be made is between the heights of the specimens (length of tubes). From the data, it can be clearly seen that when the height of the specimen is higher, the value of mean crushing stress is also higher which leads to a higher tendency of absorbing the energy.

Table 4: Value of Mean Crushing Stress according to samples

<i>Samples</i>	<i>Mean Crushing Stress (MPa)</i>
CCC40	2.96
CSC40	2.75
CCC45	7.36
CSC45	5.19

Conclusion

This paper has presented the experimental results of a study to investigate the compressive behaviour of filament wound composites tubes. From the study, it shows that CCC tubes absorb higher energy compared to CSC. In relation to this, the energy absorbed by CCC40 is 27.38 % higher than CSC40 while the energy absorbed by CCC45 is 19.63 % higher than CSC45. Other results are also in favour of CCC tubes where the mean crushing stress for both CCC samples are higher compared to CSC with 7.09 % difference for 40 mm samples and 29.48 % difference for 45 mm samples. Although CCC shows better result in terms of energy absorbed, when it comes to strength to weight ratio, the CSC samples have an advantage: in terms of specific energy absorption, the value for CSC samples are 9.37 % and 6.39 % higher than CCC samples for 40 mm and 45 mm sample length respectively. This indicates that the addition of metal is effective in increasing the energy absorption capability and strength to weight ratio of composites. The CSC tube samples are lighter and have extra edges to be used in the automotive industry since nowadays, weight reduction is important due to fuel consumption factor. Other results that favour the CSC samples are the Crush Force Efficiency and crashworthiness. CSC samples achieved efficiency values nearer to 1, which is an ideal value for energy absorption. In terms of difference in length, it is clear that a longer tube gives a better energy absorption property due to its longer crush effective length in the post crushing zone.

Acknowledment

The authors would like to thank Universiti Teknologi Malaysia for funding this research and UTM Research Management Centre (RMC) for managing the research activities under Vot17H91.

References

- [1] Alias, A. and Ismail, Y. S., "Composite Materials," Universiti Teknologi Malaysia, 2003.
- [2] Carbon Fiber Market by Types, Applications, Trends & Global Forecasts (2011–2016). Retrieved on February 16, 2016, from <http://www.marketsandmarkets.com/Market-Reports/carbon-fibre-396>.
- [3] Mokhtar, I., Yahya, M. Y., Abd Kader, A. S. and Abu Hassan, S., "Experimental Analysis of Kenaf Filament Wound Tubes Under Axial Compression Load," *Applied Mechanics and Materials*, Vol. 660, 2014, pp. 778-782.
- [4] Bhatt, P. and Goel, A., "Carbon Fibres: Production, Properties and Potential Use," *Material Science Research India*, Vol. 14(1), 2017, pp. 52-57.
- [5] Schultz, M. R., "Energy Absorption Capacity of Graphite-Epoxy Composite Tubes," *Master of Science Thesis*, Virginia, 1998, pp. 115.
- [6] Huang, L., Sun, X., Yan, L. and Kasal, B., "Impact behaviour of Concrete Columns Confined by both GFRP Tube and Steel Spiral Reinforcement," *Construction and Building Materials*, Vol 131, 2017, pp. 438–448.
- [7] Palanivelu, S., Van Paeppegem, W., Degrieck, J., Kakogiannis, D., Van Ackeren, J., Van Hemelrijck, D., et al., "Comparative Study of the Quasi-Static Energy Absorption of Small-Scale Composite Tubes with Different Geometrical Shapes for Use in Sacrificial Cladding Structures," *Polymer Testing*, 2010, 29, pp. 381–396.
- [8] Eshkoor R. A., Oshkovr, S. A., Sulong, A. B., Zulkifli, R., Ariffin, A. K., Azhar, C. H., "Effect of Trigger Configuration on the Crashworthiness Characteristic of Natural Silk Epoxy Composite Tubes," *Composites Part B*, 2013, 55, pp. 5–10.
- [9] Ochelski, S. and Gotowicki, P., "Experimental Assessment of Energy Absorption Capability of Carbon–Epoxy and Glass–Epoxy Composites," *Composites Structure*, 87, 2009, pp. 215–224.
- [10] Elgalai, A. M., Mahdi, E., Hamouda, A. M. S., Sahari, B. S., "Crushing Response of Composite Corrugated Tubes to Quasi-static Axial Loading," *Composites Structure*, 66, 2004, pp. 665–671.
- [11] Warrior, T. A., Turner, E. and Ribeaux, C. M., "Effects of Boundary Conditions on the Energy Absorption of Thin-walled Polymer Composite Tubes Under Axial Crushing," *Thin-Walled Structure*, 46, 2008, pp. 905–913.
- [12] Alkbir, M. F. M., Sapuan, S. M., Nuraini, A. A. and Ishak, M. R., "Effect

- of Geometry on Crashworthiness Parameters of Natural Kenaf Fibre Reinforced Composite Hexagonal Tubes,” *Materials & Design*, Vol. 60, 2014, pp. 85–93.
- [13] Eshkoor, R. A., Oshkovr, S. A., Sulong, A. B., Zulkifli, R., Ariffin, A. K. and Azhari C. H., “Comparative Research on the Crashworthiness Characteristics of Woven Natural Silk/Epoxy Composite Tubes,” *Material & Design*, 2013; 47, pp. 248–57.
- [14] Helaili, S., Chafra, M. and Chevalier, Y., “Hybrid Aluminum and Natural Fiber Composite Structure for Crash Safety Improvement,” *Proceedings of the TMS Middle East—Mediterranean Materials Congress on Energy and Infrastructure Systems (MEMA 2015)*. Springer International Publishing, 2016.
- [15] Ha, S. K. and Jeong, J. Y., “Effects of Winding Angles on Through-thickness Properties and Residual Strains of Thick Filament Wound Composite Rings,” *Composites Science and Technology*, Vol. 65, Issue 1, 2005, pp. 27–35.
- [16] Sapuan, S. M., Leenie, A. Harimi, M. and Beng, Y. K., “Mechanical Properties of Woven Banana Fibre Reinforced Epoxy Composites,” *Materials & Design*, Vol. 27, Issue 8, 2006, pp. 689–693.
- [17] Misri, S., Ishak, M. R., Sapuan, S. M. and Leman, Z., “The Effect of Winding Angles on Crushing Behaviour of Filament Wound Hollow Kenaf Yarn Fiber Reinforced Unsaturated Polymer Composites,” *Fibers and Polymers*, Vol. 16, 2015, pp. 2266-2275.
- [18] Abu Bakar, M. S., “CFRP-Honeycomb Sandwich Structure Tube Under Compressive Load,” *Final Year Project*, Universiti Teknologi Malaysia, 2005.
- [19] Mamalis, A. G, Robinson, M., Manolakos, D. E., Demosthenous, G. A., Ioannidis M. B. and Carruthers, J., “Energy Absorption Capability of Fibreglass Composite Square Frusta Subjected to Static and Dynamic Axial Collapse,” *Composite Structures*, 37, 1997, pp. 109-134.
- [20] Barnes, G., “Crash Safety Assurance Strategies for Future Plastic and Composite Intensive Vehicles (PCIVS),” Paperback, *Create Space Independent Publishing Platform*, June 30, 2010.